18

Copper-doped carbon nanoparticles as a two-modal nanoprobe for luminescent and magnetic resonance imaging

© E.A. Stepanidenko[1,¶], A.A. Vedernikova[1], S.O. Ondar[1,2], Z.F. Badrieva[3], E.A. Brui[3], M.D. Miruschenko[1], O.V. Volina[4], A.V. Koroleva[4], E.V. Zhizhin[4], E.V. Ushakova[1]

[1] International Scientific and Educational Center for Physics of Nanostructures, ITMO University, 197101 St. Petersburg, Russia
[2] St. Petersburg State Technological Institute (Technical University), 190013 St. Petersburg, Russia
[3] Faculty of Physics, ITMO University, 197101 St. Petersburg, Russia
[4] Research Park, St. Petersburg State University, 199034 St. Petersburg, Russia

[¶]e-mail: eastepanidenko@itmo.ru

Received May 05, 2023
Revised May 26, 2023
Accepted May 26, 2023

In this work, copper-doped carbon nanoparticles with emission in a wide spectral range and the ability to change the relaxation times of water protons during magnetic resonance imaging were fabricated. A high relaxivity value $r1 = 0.92\,mM^{-1}\cdot s^{-1}$ was achieved, which is the highest value of r1 for copper nanoparticles, to our knowledge. The suggested carbon nanoparticles are promising two-modal nanoprobes for bioimaging.

Keywords: carbon nanoparticles, long-wavelength photoluminescence, magnetic resonance imaging, contrast agents.

DOI: 10.61011/EOS.2023.07.57137.4983-23

Introduction

Luminescent carbon nanoparticles belong to a large class of modern carbon nanomaterials, active research into which is gaining popularity every year. This interest of scientists is associated with the ability to control the morphology and optical properties of carbon nanoparticles by varying the synthesis methods and types of precursors used, as well as using various post-synthetic processing procedures. In addition, carbon nanoparticles are a biocompatible and low-toxic nanomaterial, which makes their production safe and environmentally friendly. All these advantages of carbon nanoparticles allow them to be used in various fields: photonics and optoelectronics [1–3], analytical chemistry [4–6], security coding [7–9] and biomedicine [10,11].

A particularly important area of research is the creation of luminescent samples based on carbon nanoparticles for bioimaging. The development of particles with optical transitions in the red and near-infrared (IR) spectral region is relevant, since this range falls within the transparency window of biological tissues, and the photoluminescence (PL) quantum yield (QY) of carbon particles in this range usually does not exceed several percent [12,13]. In our previous study, nanoparticles based on an IR dye with PL at 1085 nm were developed with a maximum PL QY of 0.2% at that time [14]. In the paper [15] high values of the PL QY of aqueous solutions up to 21.9% were achieved for carbon dots from citric acid (CA) and formamide, which were effectively used for luminescent bioimaging. In addition, it has been shown that carbon nanoparticles with long-wavelength PL can be used for simultaneous imaging and treatment of diseases [16].

Another effective imaging method is magnetic resonance imaging (MRI), which is based on recording and spatially encoding the nuclear magnetic resonance signal, mainly from water protons. The contrast between tissues in MRI is due to differences in longitudinal (T1) and transverse (T2) relaxation times, as well as proton density. Native contrast between healthy and pathological tissues is not always sufficient for visual analysis. To increase the contrast of individual tissues, contrast agents are used — preparations based on paramagnetic or transition metals containing unpaired electrons in the outermost shell (gadolinium Gd, manganese Mn, dysprosium Dy, etc.), which are capable of changing the T1 and/or T2 times in given tissues [17]. The main characteristic of contrast agents is relaxivity (r), which reflects how the relaxation rates R1 or R2 depend on their concentration. Today, most contrast agents used in practice contain Gd; they are effective and well studied, but have some disadvantages such as high cost and potential side effects [18].

A search is underway for more accessible, cheaper and safer materials to replace Gd-based contrast agents. The paramagnetic copper ion Cu^{2+} contains an unpaired $3d$ electron and is promising for the development of cheaper contrast agents. To date, there are still few works devoted to the study of copper-based materials;

micro- and nanoparticles and complex compounds based on iron or manganese are more popular [19]. Thus, the relaxivity values r1 of most copper-based nanoparticles were maximum $0.5\,mM^{-1}\cdot s^{-1}$ [20,21]. In paper [22], polyacrylic acid nanoparticles coated with $Cu_2(OH)PO_4$ were proposed, which were effective for simultaneous IR and MR imaging, cancer therapy, where the longitudinal relaxivity r1 reached $0.62\,mM^{-1}\cdot s^{-1}$. The highest value of $r1 = 0.7331\,mM^{-1}\cdot s^{-1}$, as far as we know, was obtained in a recent study for dendrimers with Cu(II), which were used as a contrast agent, a luminescent probe, and also for chemodynamic cancer therapy [23].

The formation of multimodal nanoprobes based on carbon nanoparticles, applicable for both PL and MR imaging, is a promising and insufficiently studied area. Doping nanoparticles with paramagnetic or transition metals allows to create such multifunctional systems that combine the unique photophysical properties of carbon nanoparticles and the ability of the proposed metals to influence the relaxation properties of protons. The literature reports on bimodal nanoprobes based on carbon nanoparticles doped with Gd [24–27], lanthanides [28–30], Mn [31 –34]. There are also several papers where Cu-doped carbon nanoparticles were proposed, but the authors studied their use as highly sensitive optical sensors in analytical chemistry [6,35,36] and platforms for monitoring catalytic processes [37], for photothermal cancer therapy [36], etc. Thus, to the best of our knowledge, studies of such structures as bimodal nanoprobes for luminescence and MR imaging have not yet been carried out.

In this paper, CD−Cu carbon nanoparticles doped with copper ions and exhibiting luminescence in the blue-green (420−530 nm) and red (600 nm) spectral regions were synthesized. The resulting CD−Cu sample was examined for the opportunity of using it as a contrast agent during T1 and T2 MRI: a change in relaxation times was observed in the presence of CD−Cu. In addition, the relaxivity values r1 and r2 were calculated, which were 0.92 and $2.66\,mM^{-1}\cdot s^{-1}$. Thus, in this paper, the highest value of relaxivity r1 was obtained for nanoparticles with copper. The obtained optical properties, together with the results of MR scanning, confirm the possibility of using these particles as a bimodal nanoprobe for bioimaging.

Materials and research methods

Materials

The following solvents were used in the study: formamide ($\geq$ 99.0%, ReagentPlus, GC, Sigma-Aldrich, Germany), ethanol (98%, Lenreaktiv, Russia). Reagents: citric acid (CA, $\geq$ 99.5%), copper (II) chloride dihydrate ($CuCl_2$, $\geq$ 99.99%). All chemical reagents were used as obtained. Saline solution 0.9% (SOLOPHARM, Grotex, Russia) was used as a solvent when recording MRI. Deionized (DI) water (Milli-Q water) was used in the experiments.

Synthesis of carbon nanoparticles

Copper-doped carbon nanoparticles were prepared by a one-step solvothermal method. For this, 0.5 g of CA and 0.127 g of $CuCl_2$ were dissolved in 5 ml of formamide. The mixture of precursors was stirred until completely dissolved and placed in stainless steel autoclaves with Teflon coating and heated at 180 ° C for 12 h. After the reaction, the autoclave was naturally cooled to room temperature. To remove unreacted precursors and molecular fluorophores, the resulting solution was dissolved in 30 ml of ethanol and precipitated by centrifugation at 6,000 rpm for 15 min. This procedure was repeated 3 times until the supernatant changed color from dark red to light purple, then the precipitates were dissolved in DI water and dialyzed (Molecular weight cut-off (MWCO) 3.5 kDa) against DI water for 24 h. The resulting solution of nanoparticles after dialysis was centrifuged at 6,000 rpm for 5 min to remove large aggregates. The resulting sample was named as CD−Cu.

Research methods

The sample sizes were analyzed by atomic-force microscopy (AFM) on a Solver PRO-M microscope (NT-MDT, Russia) in semi-contact mode. Infrared (IR) spectra with Fourier transform were obtained on a Tenzor II spectrophotometer (Bruker, USA). For the elemental analysis of the resulting nanoparticles, the method of X-ray photoelectron spectroscopy (XPS) was used, which was carried out using an ESCALAB 250Xi photoelectron spectrometer (Thermo Fisher Scientific, USA) (AlKα radiation, photon energy 1486.6 eV). The metal content of carbon nanoparticles was determined by inductively coupled plasma optical emission spectrometry (ICP-OES) using a ICPE-9000 spectrometer (Shimadzu, Japan). To carry out MRI analysis, carbon nanoparticles were dissolved in 0.9% saline solution with different metal ion concentrations in the range 0−1 mM. Relaxation was measured using a clinical MRI scanner with a field of 1.5 T (Magnetom Espree, Siemens Helthineers, Germany). The relaxivity values (r1, r2) were calculated from the slopes of linear approximations of the dependences of the relaxation rates (1/T1 and 1/T2) on the metal content in the samples. The absorption spectrum of the solution was obtained on a UV-3600 spectrophotometer (Shimadzu, Japan); PL intensity distribution maps depending on the excitation wavelength of the sample (PLE-PL maps) were recorded on a Cary Eclipse spectrofluorimeter (Agilent, USA).

Results and discussion

The morphology of the resulting carbon nanoparticles was studied by AFM; the resulting image is presented in Fig. 1, *a* along with the height distribution. The average height of nanoparticles was 2.3 ± 1.1 nm, while the sizes of CD−Cu did not exceed 10 nm. The chemical composition

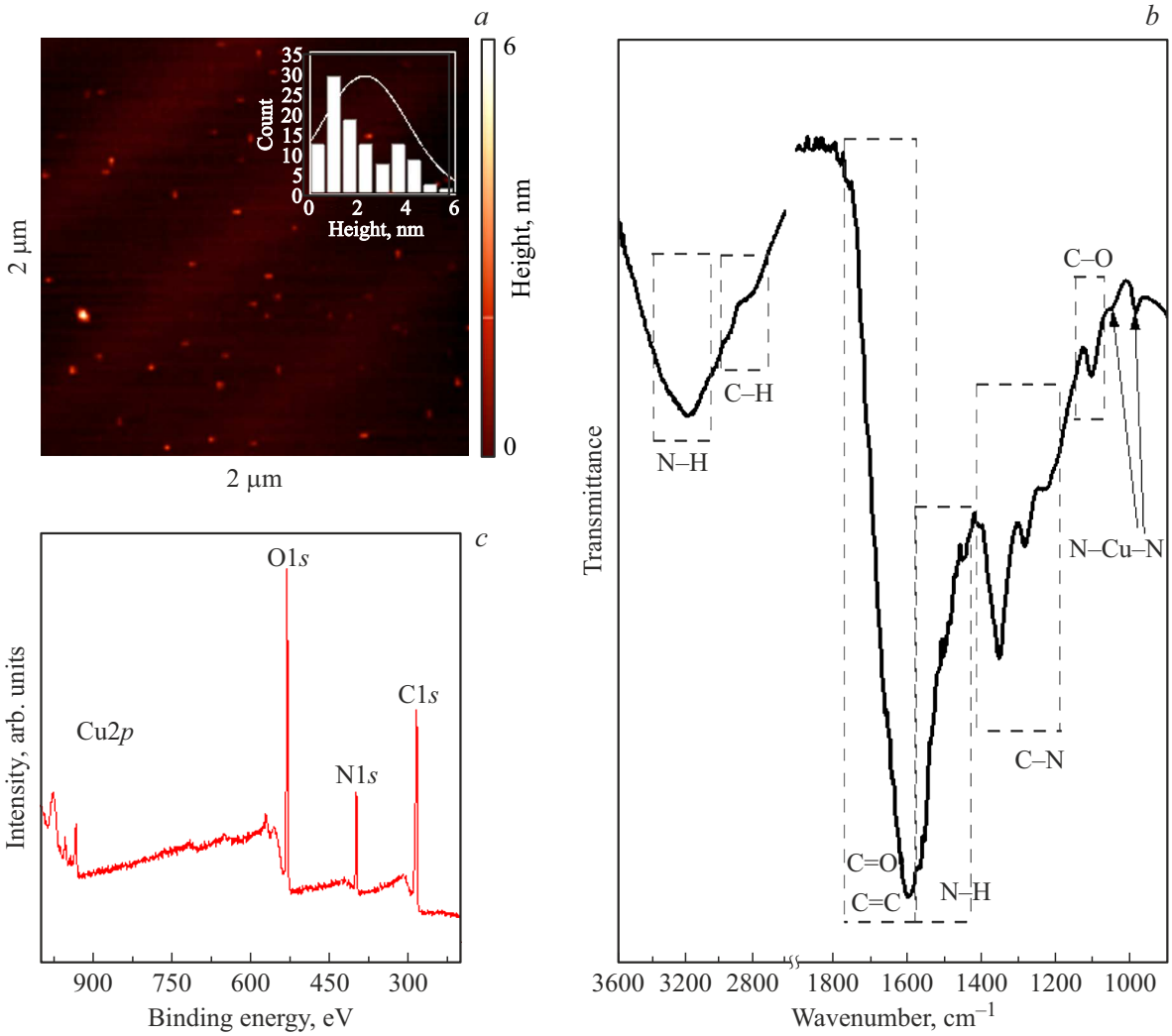

Figure 1. Studies of CD−Cu morphology: AFM image with dimensions $2 \times 2\,\mu$m (a), the inset shows the corresponding distribution of nanoparticle heights. Fourier-transform IR spectrum of CD−Cu (b), the characteristic vibration bands of different groups are highlighted by rectangles and labeled. Survey XPS spectrum of CD−Cu (c).

of the sample was studied using Fourier-transform infrared spectroscopy (Fig. 1, *b*). The peaks at 2820 and 2956 cm^{-1} are attributed to the vibrations of aliphatic groups C−H. The absorption area in the range of 1680−1500 cm^{-1} with peaks around at 1600 and 1568 cm^{-1} can be attributed to the stretching and bending vibrations of amide I (C = O) and amide II (N−H) respectively. In addition, intense absorption in the region of 1700− 1650 cm^{-1} can also be caused by the vibration of C = O bonds of carboxyl groups along with the formation of C = C bonds of the aromatic system (aromatic carbon domains in sp^2 hybridization). The peak at 1350 cm^{-1} in the spectrum of CD−Cu belongs to the C−N groups in the secondary amine associated with aromatic carbon domains. Peaks at 1282, 1221 and 1100 cm^{-1} may indicate the presence of (NH) C = O groups and C−O vibrations inside carbon nanoparticles, respectively. The peaks at 1045 and 983 cm^{-1} can be attributed to the stretching vibrations N−Cu−N [38]. Thus, the CD−Cu sample exhibits a high content of aromatic carbon domains, as well as secondary amines and amides. Next, an XPS analysis of the sample was carried out; Fig. 1, *c* shows a survey XPS spectrum. The table shows the atomic percent of C, N, O, and Cu in the CD−Cu sample.

Table 1. Atomic ratio of C, N, O, Cu atoms calculated from XPS analysis

Element	Atomic %
C	56.8
O	28.1
N	13.5
Cu	1.5

High-resolution XPS spectra for the C 1*s*, N 1*s*, O 1*s* and Cu 2*p* bands and their decomposition into

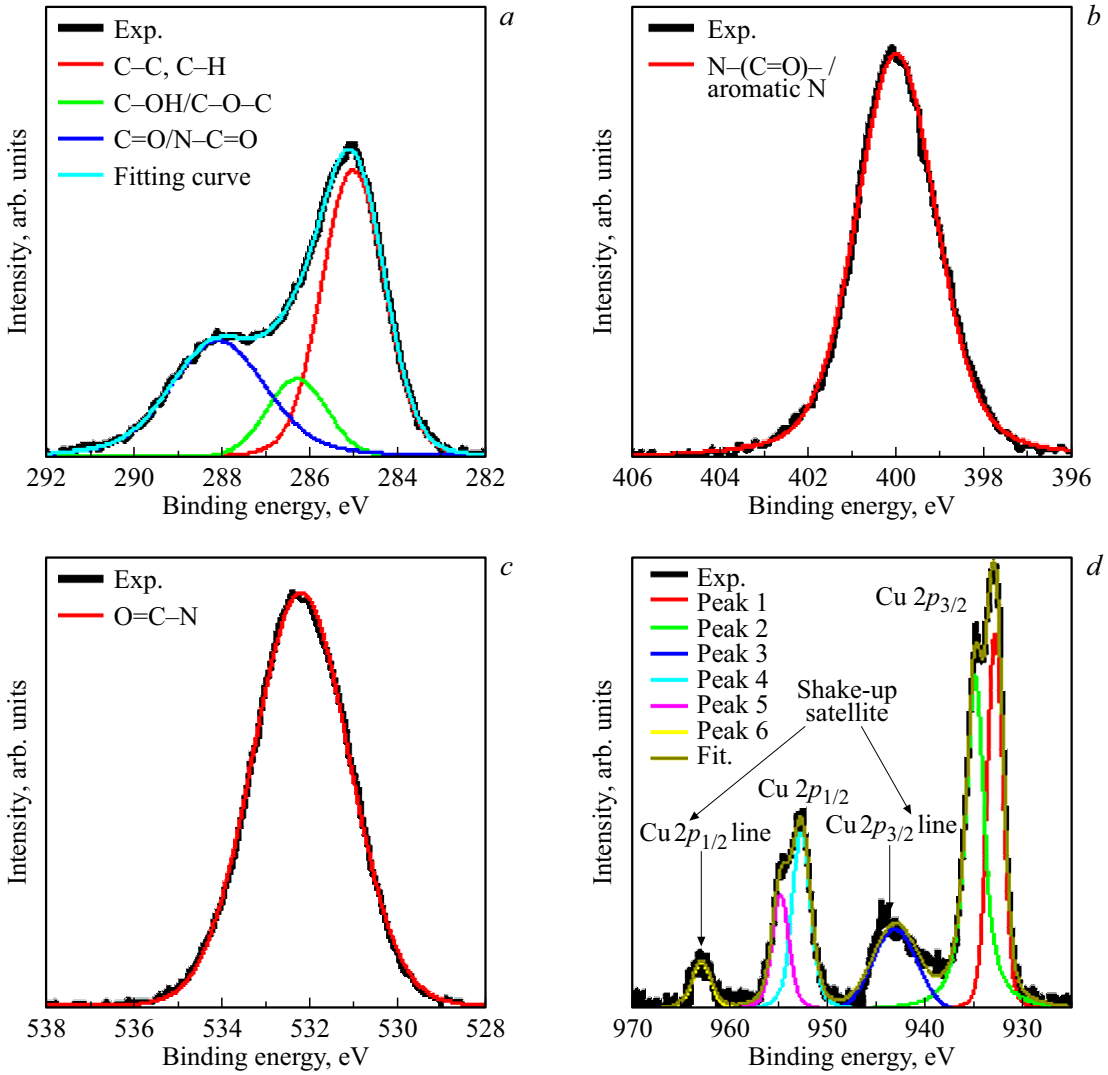

Figure 2. High resolution XPS spectra: (*a*) C 1*s*, (*b*) N 1*s*, (*c*) O 1*s*, (*d*) Cu 2*p*.

peaks corresponding to various bonds are presented in Fig. 2. Band C 1*s* (Fig. 2, *a*) consists of peaks around 285, 286.5 and 288.4 eV, which belong to C−C/C−H, C−OH/C−O−C/C−N and R−C = O bonds, respectively From the spectrum for N 1*s* (Fig. 2, *b*) it is clear that nitrogen is also part of the N−C = O groups and is associated with aromatic carbon domains. Oxygen is also found mainly in the N−C=O groups (Fig. 2, *c*). Thus, the sample contains a significant content of N−C = O groups. The spectrum of Cu 2*p* shows two bands Cu $2p_{3/2}$ and Cu $2p_{1/2}$ in the area 932.9−934.9 and 952.7−954.8 eV, respectively, and satellite bands (Fig. 2, *d*). This type of XPS spectrum indicates a predominant content of copper Cu (II) (*2, 3, 5, 6* in Fig. 2, *d*), with a small content Cu (I) (*1, 4* in Fig. 2, *d*).

Figure 3 shows the optical properties of the CD−Cu sample. In the absorption spectrum (Fig. 3, *a*) there is a monotonic increase in optical density in the range of 200−300 nm, which is associated with the formation of C = C bonds and optical transitions of the carbonized core. According to the paper [39], absorption in the area of 300−450 nm and a wide absorption band at 500−600 nm with a maximum at ≈ 520 nm are due to transitions in optical centers based on N/O-doped polycyclic aromatic hydrocarbons (PAH) and their derivatives in the cores of carbon nanoparticles and on their surface, respectively. The monotonically decreasing absorption in the region of 600−700 nm can be associated with optical $n - \pi^*$ transitions of surface molecular groups associated with sp^2 domains. On the PLE-PL map (Fig. 3, *b*) there is a PL band depending on the excitation wavelength, with a peak shifting from 420 to 530 nm when the excitation wavelength changes from 350 to 430 nm. The position of the long-wavelength PL peak does not depend on excitation and is observed at 620 nm upon excitation with a wavelength of 550 nm. From a comparison of absorption bands and excitation peaks, it is clear that the blue-green PL is due to various doped PAHs inside the particles, and the red PL

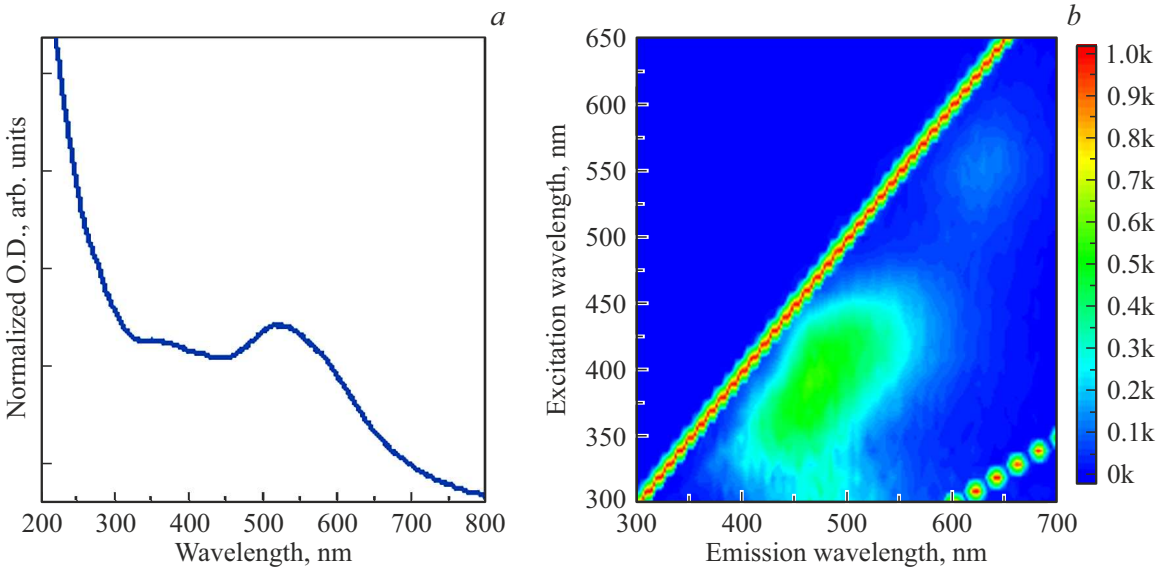

Figure 3. Absorption spectrum (a) and PLE–PL map (b) of an aqueous solution of CD–Cu.

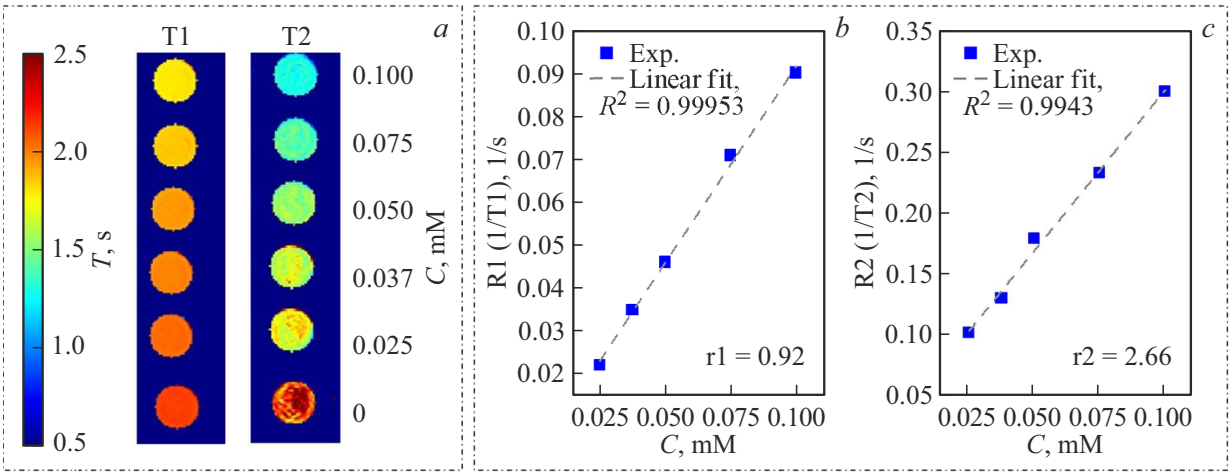

Figure 4. MRI characteristics of CD–Cu: (a) T1- and T2-maps obtained from MRI of samples with CD–Cu; (b) dependence of the longitudinal R1 (1/T1) and (c) transverse R2 (1/T2) relaxation rates on the concentration of copper ions (dashed lines indicate linear approximation). The calculated relaxivities (r1, r2) are shown in the graphs (b) and (c).

band is due to electronic transitions on the surface of the nanoparticles [39].

The carbon nanoparticles synthesized in this paper were studied *in vitro* as a contrast agent for MRI. Figure 4, *a* shows T1- and T2-maps of the samples and the dependences of the relaxation rates (R1, R2) calculated from them on the metal concentration in the sample (solutions of CD–Cu in 0.9% saline solution) (Fig. 4, *b*). As can be seen from the T1/T2-maps, the synthesized CD–Cu is able to act as a contrast agent and reduce T1 and T2. The values of the corresponding relaxivities r1 and r2, calculated as the slope of the curve of the dependence of the relaxation rate on the metal concentration, are equal to 0.92 and 2.66 $mM^{-1} \cdot s^{-1}$, respectively.

It is believed that the ratio r2/r1 determines the type of contrast agent: if r2/r1$\leq$ 5, then the substance under study is classified as a positive or T1 contrast agent, if the ratio is higher than 10 — negative or T2 contrast agents [40]. For the nanoparticles synthesized in this paper, the ratio is r2/r1 = 2.9, which indicates the prospect of using these nanoparticles as T1 contrast agents.

Conclusion

Herein citric acid-based nanoparticles doped with copper, emissive in a wide spectral range, including red, and promising as luminescent nanoprobes for bioimaging have been successfully developed. It was also found that the resulting

carbon nanoparticles are able to change the relaxation times of water protons during MRI, and the calculated relaxivity r1 reached $0.92\,mM^{-1}\cdot s^{-1}$, which is the highest value for copper-based contrast agents, to our knowledge. Although commercial gadolinium-based contrast agents have higher relaxivities, the proposed nanoparticles can be a safe, cheap and effective replacement for existing contrast agents. Thus, the obtained results make an important contribution to the development of multifunctional nanoprobes based on carbon nanoparticles.

Acknowledgments

The authors express their gratitude to the ITMO University Core Facility Center „Nanotechnologies“ XPS and ICP-OES studies were carried out on the equipment of the Resource Centers „Physical Methods of Surface Investigation“ and „Chemical Analysis and Materials“ of the St. Petersburg State University Scientific Park, respectively. MRI studies were performed using the equipment of St. Petersburg State University and the National Medical Research Center named after V.A. Almazov.

Funding

The paper was supported financially by a grant from the Russian Science Foundation (RSF) № 22.73.00090, https://rscf.ru/project/22-73-00090/. Part of the work devoted to MRI experiments was supported by a grant from the scientific school НШ-2359.2022.4. E.V.U, A.A.V and M.D.M. thank the Federal Academic Leadership Program „Priority 2030“ for financial support.

Conflict of interest

The authors declare that they have no conflict of interest.

References

[1] A.P. Litvin, X. Zhang, E.V. Ushakova, A.L. Rogach. Adv Funct Mater, **31** (18), 2010768 (2021). DOI: 10.1002/adfm.202010768
[2] E.A. Stepanidenko, E.V. Ushakova, A.V. Fedorov, A.L. Rogach. Nanomaterials, **11** (2), 364 (2021). DOI: 10.3390/nano11020364
[3] P.P. Falara, A. Zourou, K.V. Kordatos. Carbon NY, **195**, 219 (2022). DOI: 10.1016/j.carbon.2022.04.029
[4] T. Rasheed. TrAC Trends in Analytical Chemistry, **158**, 116841 (2023). DOI: 10.1016/j.trac.2022.116841
[5] Z. Wang, L. Zhang, K. Zhang, Y. Lu, J. Chen, S. Wang, B. Hu, X. Wang. Chemosphere, (2022). DOI: 10.1016/j.chemosphere.2021.132313
[6] X. Xu, Z. Chen, Q. Li, D. Meng, H. Jiang, Y. Zhou, S. Feng, Y. Yang. Microchemical J., **160** (2021). DOI: 10.1016/j.microc.2020.105708
[7] K. Jiang, Y. Wang, C. Cai, H. Lin. Advanced Materials, **30** (26), 1800783 (2018)
[8] Z. Tian, D. Li, E.V. Ushakova, V.G. Maslov, D. Zhou, P. Jing, D. Shen, S. Qu, A.L. Rogach. Advanced Science, **5** (9), 1800795 (2018). DOI: 10.1002/advs.201800795
[9] Y. Ding, X. Wang, M. Tang, H. Qiu. Advanced Science, **9** (3) (2022). DOI: 10.1002/advs.202103833
[10] W. Su, H. Wu, H. Xu, Y. Zhang, Y. Li, X. Li, L. Fan. Mater. Chem. Front., **4** (3), 821 (2020). DOI: 10.1039/c9qm00658c
[11] S. Khan, A. Dunphy, M.S. Anike, S. Belperain, K. Patel, N.H.L. Chiu, Z. Jia. International J. Molecular Sciences, **22** (13), 6786 (2021). DOI: 10.3390/IJMS22136786
[12] D. Li, E.V. Ushakova, A.L. Rogach, S. Qu. Small, **17** (43), 2102325 (2021). DOI: 10.1002/SMLL.202102325
[13] H. Ding, X.X. Zhou, J.S. Wei, X.B. Li, B.T. Qin, X.B. Chen, H.M. Xiong. Carbon NY, (2020). DOI: 10.1016/j.carbon.2020.06.024
[14] E.A. Stepanidenko, I.D. Skurlov, P.D. Khavlyuk, D.A. Onishchuk, A.V. Koroleva, E.V. Zhizhin, I.A. Arefina, D.A. Kurdyukov, D.A. Eurov, V.G. Golubev, A.V. Baranov, A.V. Fedorov, E.V. Ushakova, A.L. Rogach. Nanomaterials, **12**(3) (2022). DOI: 10.3390/nano12030543
[15] H. Zhang, G. Wang, Z. Zhang, J.H. Lei, T.M. Liu, G. Xing, C.X. Deng, Z. Tang, S. Qu. Light: Science & Applications, **11** (1), 1 (2022). DOI: 10.1038/s41377-022-00798-5
[16] M. Zheng, Y. Li, S. Liu, W. Wang, Z. Xie, X. Jing. ACS Appl Mater Interfaces, **8** (36), 23533 (2016). DOI: 10.1021/acsami.6b07453
[17] Y.D. Xiao, R. Paudel, J. Liu, C. Ma, Z.S. Zhang, S.K. Zhou. Int J. Mol. Med., **38** (5), 1319 (2016). DOI: 10.3892/IJMM.2016.2744/HTML
[18] Hazardous Substances Data Bank (HSDB: 7547 - PubChem. Available at: https://pubchem.ncbi.nlm.nih.gov/source/hsdb/7547. Accessed April 6, 2023
[19] D. Zhuang, H. Zhang, G. Hu, B. Guo. J. Nanobiotechnology, **20** (1), 1 (2022). DOI: 10.1186/S12951-022-01479-6
[20] O. Perlman, I.S. Weitz, H. Azhari. Phys. Med. Biol., **60** (15), 5767 (2015). DOI: 10.1088/0031-9155/60/15/5767
[21] O. Perlman, A. Borodetsky, Y. Kauffmann, Y. Shamay, H. Azhari, I.S. Weitz. ACS Appl. Nano Mater., **2** (10) (2019). DOI: 10.1021/acsanm.9b00791
[22] Y. Chen, P. Liu, P. Sun, J. Jiang, Y. Zhu, T. Dong, Y. Cui, Y. Tian, T. An, J. Zhang, Z. Li, X. Yang. Theranostics, **9** (5), 1453 (2019). DOI: 10.7150/THNO.29987
[23] C. Song, Z. Ouyang, Y. Gao, H. Guo, S. Wang, D. Wang, J. Xia, M. Shen, X. Shi. Nano Today, **41** (2021). DOI: 10.1016/j.nantod.2021.101325
[24] H. Chen, Y. Qiu, D. Ding, H. Lin, W. Sun, G.D. Wang, W. Huang, W. Zhang, D. Lee, G. Liu, J. Xie, X. Chen. Advanced Materials, **30** (36) (2018). DOI: 10.1002/adma.201802748
[25] S. Zheng, N. Yu, C. Han, T. Xie, B. Dou, Y. Kong, F. Zuo, M. Shi, K. Xu. Biochem. Biophys. Res. Commun., **511** (2), 207 (2019). DOI: 10.1016/j.bbrc.2019.01.098
[26] Y. Huang, L. Li, D. Zhang, L. Gan, P. Zhao, Y. Zhang, Q. Zhang, M. Hua, C. Jia. Magn. Reson. Imaging, **68**, 113 (2020). DOI: 10.1016/j.mri.2020.02.003
[27] L. Cardo, L. Martínez-Parra, M. Cesco, B.M. Echeverría-Beistegui, M. Martínez-Moro, N. Herrero-Álvarez, M. Cabrerizo, S. Carregal-Romero, P. Ramos-Cabrer, J. Ruiz-Cabello, M. Prato. Small, 2206442 (2023). DOI: 10.1002/smll.202206442
[28] G.K. Das, N.J.J. Johnson, J. Cramen, B. Blasiak, P. Latta, B. Tomanek, F.C.J.M. van Veggel. J. Phys. Chem. Lett., **3** (4), 524 (2012). DOI: 10.1021/jz201664h

[29] T. Samanta, C. Hazra, V. Mahalingam. New J. Chemistry, **39** (1), 106 (2015). DOI: 10.1039/C4NJ01647E
[30] F. Wu, L. Yue, L. Yang, K. Wang, G. Liu, X. Luo, X. Zhu. Colloids Surf. B: Biointerfaces, **175** (2019). DOI: 10.1016/j.colsurfb.2018.11.054
[31] Z. Ji, P. Ai, C. Shao, T. Wang, C. Yan, L. Ye, W. Gu. ACS Biomater. Sci. Eng., **4** (6), 2089 (2018). DOI: 10.1021/acsbiomaterials.7b01008
[32] Q. Jia, J. Ge, W. Liu, X. Zheng, S. Chen, Y. Wen, H. Zhang, P. Wang. Advanced Materials, **30** (13) (2018). DOI: 10.1002/adma.201706090
[33] M. Zhang, T. Zheng, B. Sheng, F. Wu, Q. Zhang, W. Wang, J. Shen, N. Zhou, Y. Sun. Chemical Engineering J., **373** (2019). DOI: 10.1016/j.cej.2019.05.107
[34] S. Sun, L. Zhao, D. Wu, H. Zhang, H. Lian, X. Zhao, A. Wu, L. Zeng. ACS Appl. Bio. Mater., **4** (2), 1969 (2021). DOI: 10.1021/acsabm.0c01597
[35] P.P. Zhu, Z. Cheng, L.L. Du, Q. Chen, K.J. Tan. Langmuir, **34** (34), 9982 (2018). DOI: 10.1021/acs.langmuir.8b01230
[36] Y. Liu, P. Wu, X. Wu, C. Ma, S. Luo, M. Xu, W. Li, S. Liu. Talanta, **210** (2020). DOI: 10.1016/j.talanta.2019.120649
[37] M. Najaflu, M. Shahgolzari, F. Bani, A.Y. Khosroushahi. ACS Omega, **7** (38), (2022). DOI: 10.1021/acsomega.2c04484
[38] J. Du, Y. Zhao, J. Chen, P. Zhang, L. Gao, M. Wang, C. Cao, W. Wen, C. Zhu. RSC Adv, **7** (54) (2017). DOI: 10.1039/c7ra05383e
[39] B. Zhang, B. Wang, E.V. Ushakova, B. He, G. Xing, Z. Tang, A.L. Rogach, S. Qu. Small, 2204158 (2022). DOI: 10.1002/smll.202204158
[40] S. Caspani, R. Magalhães, J.P. Araújo, C.T. Sousa. Materials, **13** (11), 2586 (2020). DOI: 10.3390/ma13112586

Translated by E.Potapova